Mild Preoxidation Treatment of Pt/TiO$_2$ Catalyst and Its Enhanced Low Temperature Formaldehyde Decomposition

Kangzhong Shi [1,2], Lei Wang [1,3], Long Li [1], Xuejuan Zhao [4,*], Yuanyuan Chen [1], Zelin Hua [1], Xiaobao Li [1], Xiaoli Gu [1] and Licheng Li [1,5,*]

[1] Innovation Research Center of Lignocellulosic Functional Materials, College of Chemical Engineering, Nanjing Forestry University, Nanjing 210037, China
[2] Eastman Shuangwei Fibers Company Limited, Hefei 230601, China
[3] Research Institute of Wison Advanced, Wison (China) Holding Company, Shanghai 201210, China
[4] School of Materials Science and Engineering, Nanjing Institute of Technology, Nanjing 211167, China
[5] State Key Laboratory of Materials-Oriented Chemical Engineering, Nanjing Tech University, Nanjing 210009, China
[*] Correspondence: zhaoxj@njit.edu.cn (X.Z.); lilc@njfu.edu.cn (L.L.)

check for updates

Abstract: The typical platinum nanoparticles loaded on titania (Pt/TiO$_2$) were pretreated with mild oxidation (<300 °C) in pure oxygen to enhance the low-temperature formaldehyde (HCHO) decomposition performance. The structural properties of support and platinum nanoparticles were characterized by X-ray diffraction (XRD), physical adsorption/desorption, high-resolution transmission electron microscopy (HRTEM), in situ diffuse reflectance infrared Fourier transform spectroscopy (DRIFITS), and temperature-programmed reduction and oxidation (TPR and TPO). The catalytic results showed that the low temperature HCHO decomposition activity of mild pre-oxidized Pt/TiO$_2$ was around three times that of the pristine one. According to the characterization results, the structure of the Pt/TiO$_2$ support and their Pt particle sizes had negligible change after pre-oxidation treatment. The cationic Pt content of Pt/TiO$_2$ and surface roughness of Pt nanoparticles gradually increased with the increasing temperature of the pre-oxidation treatment. Mild pre-oxidation treatment was beneficial to the oxygen activation and water dissociation of Pt/TiO$_2$. In situ HCHO-DFIRTS results showed that the mild pre-oxidation treatment could enhance the dehydrogenation of formate.

Keywords: formaldehyde; platinum; mild peroxidation; TiO$_2$; catalytic decomposition

1. Introduction

Formaldehyde (HCHO) is one of the most typical indoor pollutants. Upon long-term exposure to HCHO, the majority of people would have a heavy headache or suffer from respiratory diseases and even cancer [1]. Biodegradation, physical adsorption, and chemical reaction are three current strategies for eliminating indoor HCHO [2]. Sustainability and environmental friendliness gradually become two requirements for developing novel air purification technologies. Among them, low-temperature catalytic oxidation is one of the chemical reaction approaches, which could spontaneously decompose HCHO into CO$_2$ and H$_2$O [3–5]. Noble metal catalysts, e.g., Pt, Pd, and Rh, have become the keystone of low-temperature catalytic oxidation technology because of its excellent catalytic activity [4,6–9]. However, high -ost is the key factor that hinders the further application of noble metal catalysts. Therefore, to improve the catalytic performance of noble metal catalysts, it is of scientific and technological significance to reduce the economical expenditure of low-temperature HCHO decomposition.

To date, there are numerous studies on the development of effective noble metal catalysts. They could be divided into three categories: new species incorporation, support adjustment and preparation process improvement. Great progress has been achieved in the past decades [10]. Different from the other two strategies, the optimization of the preparation process does not change the original composition of the catalyst, which is usually the primary mission of catalyst development. Especially important for the thermal treatment process, it would determine the HCHO decomposition performance of noble metal catalysts due to the direct influence of their several structural parameters [10–12]. Firstly, the size of the noble metal particles was easily influenced by calcination temperature and atmosphere, which directly determined the quantity of the active sites [13]. Simultaneously, the chemical valence of noble metal particles was inevitably altered during thermal treatment [14,15]. Nowadays, there is still debate over which one, metallic or cationic Pt has the HCHO decomposition catalytic activity [4,14,16,17]. Moreover, the structural transformation of the support, along with various temperatures of thermal treatment could influence the reactant adsorption or dispersion state of the active species [18–20]. Recently, the formation mechanism from the precursor to the Pt particles was investigated in detail, and the different resulting Pt structures had various adsorption geometries of HCHO [21]. Sequentially, some novel effects of thermal treatment on the HCHO decomposition were discovered. For instance, Zhang et al. found that excessive temperature reduction may lead to the formation of strong metal-support interaction between Pd and TiO_2. This could decrease the Pd particle size and be beneficial to the activation of O_2 and water [22].

As mentioned above, the thermal treatment process significantly influences the low-temperature HCHO decomposition performance of the noble metal catalyst. However, most previous works were carried out by reducing or oxidizing the catalysts at relatively high temperature (>300 °C). Under that severe condition, the change in several structural factors, e.g., particle size and chemical valence of metals, support structure, may inter-influence the final performance of the catalyst [23]. That would increase the difficulty in dissecting their structure-performance relationship. By contrast, some attention has been focused on whether the thermal treatment under mild temperature (<300 °C) with catalysts could alter their HCHO decomposition performance. The improvement by mild thermal treatment on catalytic performance has been carried out in many other reactions, for example, CO oxidation and photocatalysis [24–27]. Different from previous research, the mild thermal treatment could mainly influence the surface structure of noble metal particles while slightly changing their bulk structures. Additionally, HCHO decomposition process contains several complex reaction steps. Therefore, it is worthy to investigate the effect of mild thermal treatment with noble catalysts on their low temperature HCHO decomposition performance.

The present work reports a mild pre-oxidation treatment for the typical Pt/TiO_2 catalyst. The low-temperature HCHO decomposition performance of the catalyst could be significantly improved by pre-oxidation treatment under pure O_2 before catalytic evaluation. The chemical valence and detailed morphological structure of Pt particles were systematically studied by various characterizations. The influence of these factors on the low-temperature HCHO decomposition performance of the catalyst was analyzed and discussed. Furthermore, in situ diffuse reflectance infrared Fourier transformed spectroscopy (HCHO-DRIFTS) was used to understand the variation in the reaction route of HCHO decomposition on different catalysts. Finally, the optimization measure of mild pre-oxidation treatment and its corresponding mechanism was clarified.

2. Results and Discussion

2.1. Formaldehyde Decomposition Performancs

Figure 1a shows the formaldehyde conversion of various catalysts as a function of reaction temperatures. At the initial stage, pristine Pt/TiO_2 has an HCHO conversion of 13.2% at 30 °C. Subsequently, the HCHO conversion of Pt/TiO_2 increases significantly when the reaction temperature goes up. The HCHO in feed gas could be completely decomposed at 100 °C for the pristine Pt/TiO_2

catalyst. In comparison, the Pt/TiO$_2$ catalysts with pre-oxidation treatment could exhibit the better performance of HCHO decomposition except Pt/TiO$_2$-O300. Noteworthy is that the Pt/TiO$_2$-O200 shows the highest HCHO conversion that could reach up to 39.6% at 30 °C. To provide quantitative comparison in the activity of various catalysts, their reaction rates at 30 °C are calculated and summarized in Figure 1b. It could be seen that Pt/TiO$_2$-O200 has nearly three times the reaction rate of the HCHO decomposition as that of pristine Pt/TiO$_2$. However, the catalytic performance of Pt/TiO$_2$ declines at the pre-oxidation temperature of 300 °C. The order of catalytic performance is as follows: Pt/TiO$_2$-O200~Pt/TiO$_2$-O100 > Pt/TiO$_2$ > Pt/TiO$_2$-O300. Obviously, this demonstrates that the mild pre-oxidation treatment, i.e., suitable temperature, could significantly improve the low-temperature HCHO decomposition performance of Pt/TiO$_2$. Moreover, the mild pre-oxidized Pt/TiO$_2$ catalyst could have an excellent catalytic stability. According to long-time catalytic test (Figure 1c), the catalyst of Pt/TiO$_2$-O200 does not show observable deactivation after 75 h. In comparison, the pristine Pt/TiO$_2$ instead has a little decrease in catalytic activity, which coincides with previous reports [16]. This implies that the improved HCHO decomposition performance of pre-oxidized Pt/TiO$_2$ is caused by their stable structural transformations rather than the oxygen species adsorption on the catalyst surface.
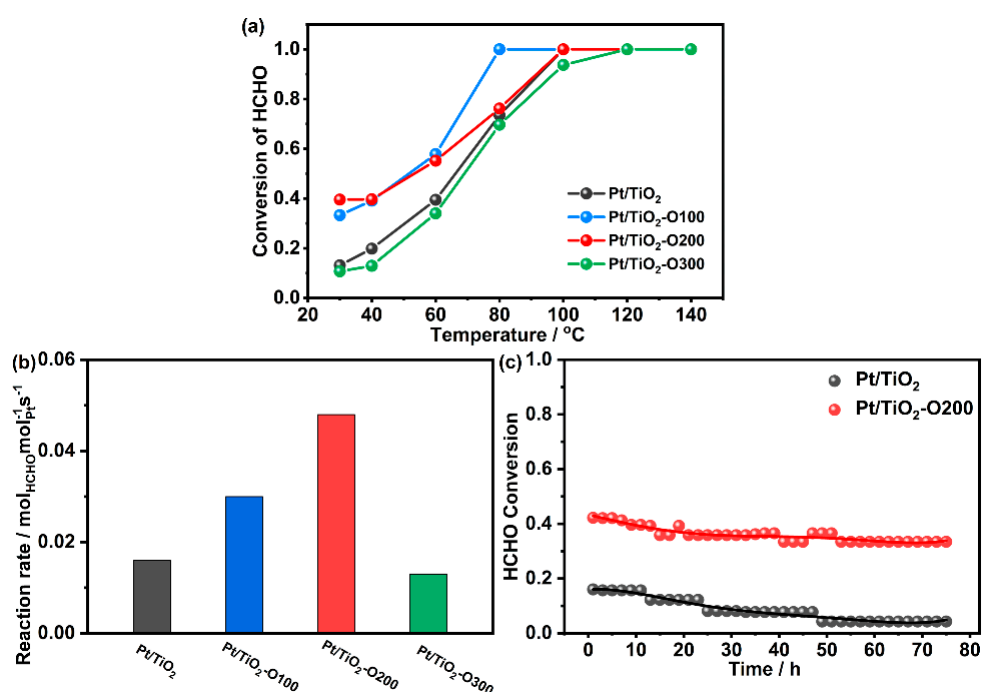

Figure 1. Formaldehyde (HCHO) conversion as a function of reaction temperature (**a**), reaction rate at 30 °C (**b**) of various Pt/TiO$_2$ catalysts, and stability test (**c**) of pristine Pt/TiO$_2$ and Pt/TiO$_2$ pre-oxidized at 200 °C.

2.2. Structural Analyses

The crystal structure of various catalysts is studied by XRD. Figure 2a shows five strong diffraction peaks at 25.4°, 37.8°, 48.0°, 53.9°, and 55.1° in all catalysts, corresponding to (101), (004), (200), (105), and (211) planes of the anatase phase [28,29], respectively. There are no signals ascribed to other phases of TiO$_2$ appearing in the XRD spectra. According to the calculation by the Scherrer equation, the crystal particle sizes of TiO$_2$ are about 19.6 ± 0.4 nm in all catalysts. This means that the structure of the TiO$_2$ framework in all catalysts does not change regardless of whether they are exposed to preoxidation treatment. Correspondingly, various pre-oxidized Pt/TiO$_2$ catalysts have a similar porous structure. As depicted in Figure 2b, the overlapped type IV N$_2$ adsorption/desorption isotherms prove the same mesoporous structure in all catalysts, as also reflected by their same pore size distributions. Their surface areas (S$_{BET}$) and pore volumes (V$_p$) listed in Table 1 are 46.0 ± 3.0 m^2/g and 0.220 ± 0.005 cm^3/g,

respectively. Moreover, no diffractive peaks of Pt species could be observed in any XRD spectra, which indicate their sufficient dispersion of Pt nanoparticles. From these detailed structural data, it could be confirmed that the mild pre-oxidation treatment does not influence the overall structure of the Pt/TiO_2 catalyst.
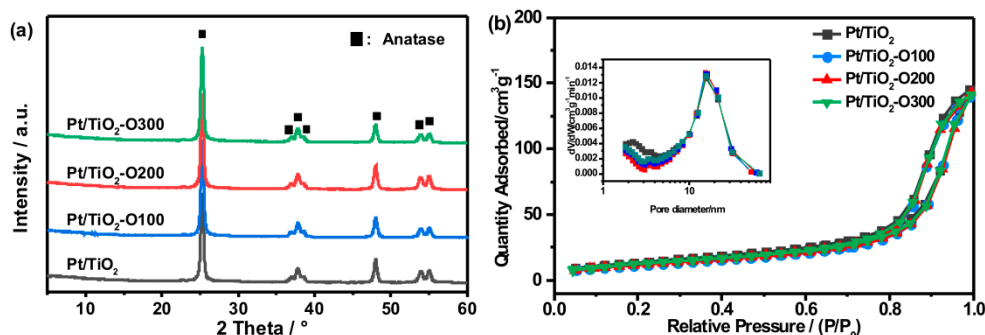

Figure 2. XRD patterns (**a**) and nitrogen adsorption/desorption isotherms (**b**) of various Pt/TiO_2 catalysts with different pre-oxidation treatments and pristine Pt/TiO_2. The inset in (**b**) is the figure of the pore size distribution of various catalysts.

Table 1. Crystal and porous structural data of various Pt/TiO_2 catalysts.

Sample	Crystal Size [a] (nm)	S_{BET} (m^2/g)	V_p (cm^3/g)	D_p (nm)
Pt/TiO_2	19.6	46.3	0.215	14.1
Pt/TiO_2-O100	20.0	43.0	0.215	14.7
Pt/TiO_2-O200	19.8	44.1	0.219	14.5
Pt/TiO_2-O300	19.2	46.8	0.218	13.9

[a]: calculated according to the Scherrer equation from the half-peak width at 25.4°.

Next, the subtler structural distinction among these Pt/TiO_2 catalysts is further carefully characterized by high-resolution transmission electron microscopy (HRTEM), X-ray Photoelectron Spectrometer (XPS), and CO diffuse reflectance infrared Fourier transformed spectroscopy (CO-DRIFTS). Figure 3a–d displays the representative HRTEM images and derived Pt particle size distributions of various Pt/TiO_2 catalysts. It can be seen that all the catalysts uniformly consist of numerous particles with dozens of nanometers, which are ascribed to TiO_2 particles. No remarkable morphological differences are observed among them. This indicates that the pre-oxidation treatment does not distinctly influence the structure of TiO_2, as consistent with the above XRD and Brunauer-Emmett-Teller (BET) analysis results. Moreover, Pt/TiO_2 contains lots of well-dispersed dark spots in the HRTEM image (Figure 3a) and bright spots in the scanning transmission electron microscopy-high-angle annular dark-field (STEM-HAADF) image (Figure 3e). According to the EDX result (Figure 3f), these spots are confirmed to be Pt nanoparticles. The statistical result shows that most probably, the Pt particle size of the pristine Pt/TiO_2 catalyst is about 2.6 nm. Under mild pre-oxidation treatment below 200 °C, the Pt/TiO_2-O100 and Pt/TiO_2-O200 exhibit around 2.7 nm of the most probable Pt particle size, which is similar to that of pristine one. That suggests the tiny influence of mild pre-oxidation treatment (<200 °C) on the structural properties of Pt nanoparticles.

In comparison, the Pt/TiO_2 catalyst pre-oxidized at 300 °C has an observable increase in the most probable Pt particle size, which reaches up to ca. 3.1 nm. The increase in Pt particle size of Pt/TiO_2-O300 may be attributed to either the Pt particle migration and coalescence or oxidation of the metallic Pt into cationic ones. According to temperature programmed oxidation (TPO) analysis result of Pt/TiO_2 in Figure 4, the profile starts to slightly upwarp at around 100 °C, which indicates the occurrence of Pt superficial oxidation. Above 200 °C, a single oxygen-consuming peak appears and the maximum peak temperature is at 310 °C. This could be ascribed to the relatively vigorous superficial oxidation of Pt nanoparticles [30]. By contrast, small Pt particles are more liable to be completely oxidized into

cationic Pt species [30]. Figure 4 also shows the temperature programmed reduction (TPR) pattern of unreduced Pt/TiO$_2$ catalyst. The signal peak appears at 83 °C, ascribed to the reduction process of cationic Pt into metallic ones [31,32]. Moreover, the broadened peak from 300 °C to 450 °C could be attributed to the reduction of the superficial lattice oxygen of titania [3,33]. Note that cationic Pt due to its amorphous form could not be imaged by TEM technology [16,34]. Hence, the observation of less Pt particles in the HRTEM image of the Pt/TiO$_2$-O300 could demonstrate the above assumption. On the other hand, it could not be excluded the tiny contribution of Pt particle migration and coalescence on the increasing Pt particle size. Wu et al. found that Pt nanoparticles did not significantly increase below 200 °C. However, Pt nanoparticles aggregate with each other as the temperature exceeds 300 °C [35]. No matter what mechanism it is, the Pt particle size of the Pt/TiO$_2$ catalyst is not significantly influenced by mild pre-oxidation treatment.
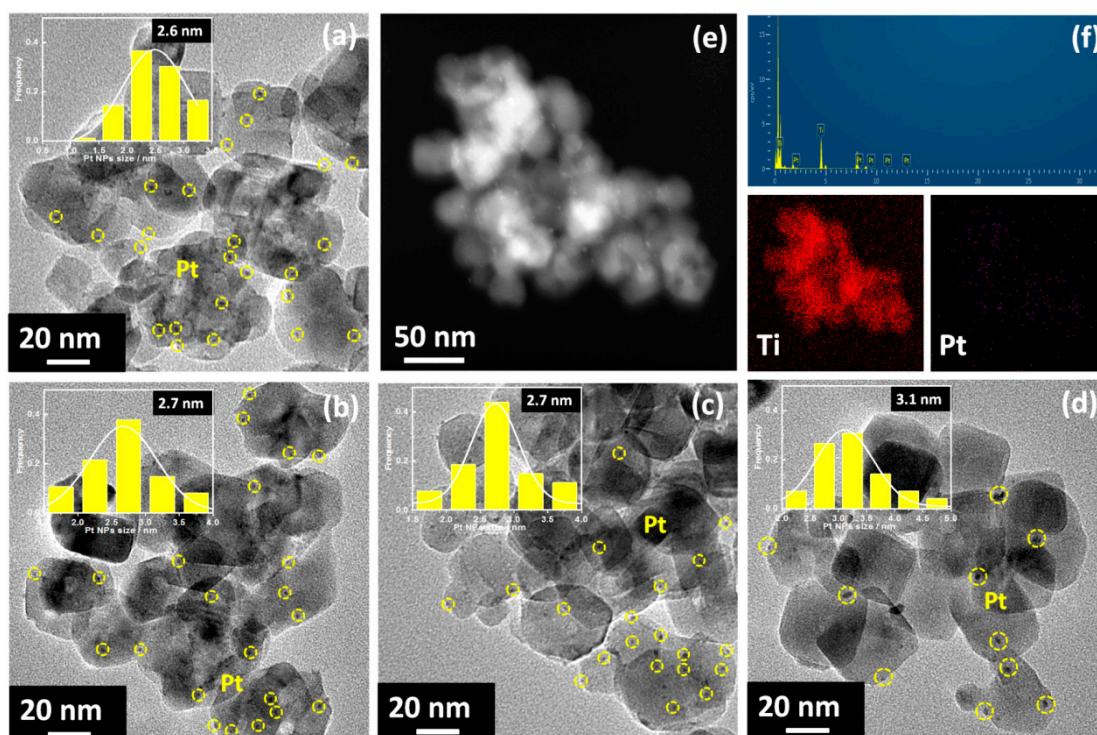

Figure 3. High-resolution transmission electron microscopy (HRTEM) images of (**a**) Pt/TiO$_2$, (**b**) Pt/TiO$_2$-O100, (**c**) Pt/TiO$_2$-O200, (**d**) Pt/TiO$_2$-O300, and a representative scanning transmission electron microscopy−high-angle annular dark-field (STEM−HAADF) image (**e**), scanning transmission electron microscopy−energy-dispersive X-ray spectroscopy STEM−EDX elemental mapping (**f**) of Pt/TiO$_2$. Inset histograms are the Pt particle size distribution of different catalysts.
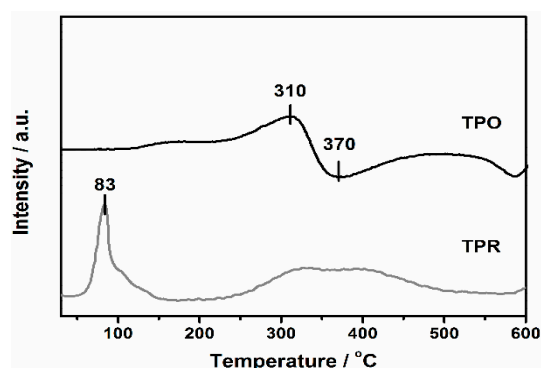

Figure 4. Temperature programmed oxidation (TPO) pattern of the pristine Pt/TiO$_2$ catalyst and temperature programmed oxidation (TPR) pattern of the unreduced Pt/TiO$_2$ catalyst.

The chemical valence state of Pt particles of various catalysts is analyzed by X-ray photoelectron spectroscopy (XPS). As plotted in Figure 5a, all the XPS Pt4*f* spectra exhibit three $4f_{7/2}$-$4f_{5/2}$ doublets at around binding energies of 70.8 eV-74.2 eV, 72.4 eV-75.7 eV and 74.0 eV-77.2 eV corresponding to Pt^0, Pt^{2+}, and Pt^{4+} species, respectively [36,37]. The area of the resolved peaks ascribed to oxidized $Pt^{\delta+}$ and metallic Pt^0 is used to estimate the content of cationic Pt in various catalysts. As listed in Table 2, the $Pt^{\delta+}/(Pt^0+Pt^{\delta+})$ values are 30.1%, 40.3%, 40.4%, and 57.3% for Pt/TiO_2, Pt/TiO_2-O100, Pt/TiO_2-O200, and Pt/TiO_2-O300, respectively. Pt/TiO_2-O100 has a similar $Pt^{\delta+}/(Pt^0 + Pt^{\delta+})$ value to that of Pt/TiO_2-O200, which is between pristine Pt/TiO_2 and Pt/TiO_2-O300. Combined with TPO analysis results, the increased $Pt^{\delta+}/(Pt^0 + Pt^{\delta+})$ value of the Pt/TiO_2-O100 and Pt/TiO_2-O200 could be attributed to the mild oxidation of surface Pt atoms. In comparison, the dramatically higher cationic Pt content of Pt/TiO_2-O300 indicates the partial oxidation of subsurface Pt atoms of Pt particles under the excessive temperature of the pre-oxidation treatment.

Furthermore, the XPS technique could also provide information about the state of the oxygen species of various Pt/TiO_2 catalysts. As shown in Figure 5b, all the catalysts have three peaks at around binding energies of 529.7 eV, 531.8 eV, and 533.5 eV, which are assigned to the lattice oxygen of bulk oxide (O_I), surface oxygen species (O_{II}), and oxygen of the surface hydroxyl (OH^-), respectively [38]. The ratio of O_{II} to O_I and OH^- to O_I is calculated to quantitatively analyze the content of oxygen species in various catalysts. As displayed in Table 2, the O_{II} content of the catalyst firstly increases and then decreases with increasing temperature of the pre-oxidation treatment. The pre-oxidized Pt/TiO_2 catalysts have obviously higher O_{II} content than that of the pristine Pt/TiO_2, especially for the that of Pt/TiO_2-O200. Moreover, the XPS signal ascribed to OH^- does not appear in the pattern of pristine Pt/TiO_2, suggesting the absence of hydroxyls. All the pre-oxidized Pt/TiO_2 catalysts have the ability of water dissociation and their OH^- contents gradually decline with increasing temperature of pre-oxidation treatment.
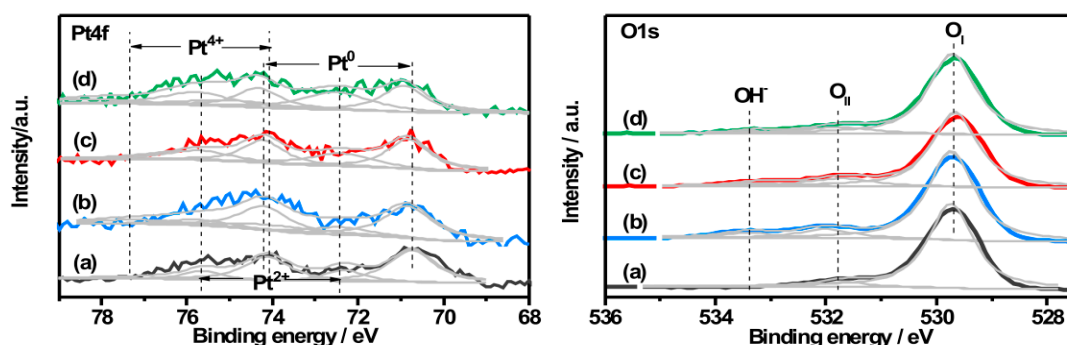

Figure 5. High-resolution XPS spectra for Pt4f and O1s of various catalysts (**a**) Pt/TiO_2, (**b**) Pt/TiO_2-O100, (**c**) Pt/TiO_2-O200, and (**d**) Pt/TiO_2-O300.

Table 2. Analyses of X-ray Photoelectron Spectrometer (XPS) and CO diffuse reflectance infrared Fourier transformed spectroscopy (CO-DRIFTS) of various pre-oxidized Pt/TiO_2 catalysts and the pristine Pt/TiO_2 catalyst.

Catalyst	BE of Pt4f$_{7/2}$ eV	$Pt^{\delta+}/(Pt^0 + Pt^{\delta+})$ %	BE of O1s eV	O_{II}/O_I	OH^-/O_I
Pt/TiO_2	70.9	30.1	529.7	0.065	<0.001
Pt/TiO_2-O100	71.1	40.3	529.5	0.121	0.066
Pt/TiO_2-O200	70.7	40.4	529.6	0.148	0.042
Pt/TiO_2-O300	70.8	57.3	529.7	0.116	0.018

The dispersion state and chemical valence of Pt nanoparticles is further characterized by in situ CO-DRIFTS. As shown in Figure 6, all the catalysts have two distinct bands at 2065 cm^{-1} and 2089 cm^{-1}, which are assigned to the CO linearly adsorbed in the Pt step and terrace sites, respectively [39]. The existence of metallic Pt has been demonstrated in all catalysts, in accordance with the XPS analysis

results. Moreover, all the pre-oxidized Pt/TiO$_2$ catalysts show one small band at 2115 cm^{-1}, which is attributed to the linear adsorption of CO onto cationic Pt species [40]. The intensity of the band seems to be promoted as the pre-oxidation temperature increases, which suggests the increasing cationic Pt content, as also consistent with the XPS analysis results.

Noteworthy is that the pristine Pt/TiO$_2$ catalyst does not show any signal to cationic Pt species. That suggests the absence of cationic Pt species in pristine Pt/TiO$_2$ catalyst. This analysis result is significantly different from 30.1% of cationic Pt species detected by XPS characterization. Herein, the existence of cationic Pt species of Pt/TiO$_2$ in the XPS analysis should be caused by the exposure in air or oxidation by O$_2$ and moisture during the transfer of the catalyst to the XPS chamber. According to the above TPR result (Figure 4), the present reduction in temperature of the Pt/TiO$_2$ catalyst preparation (300 °C) could guarantee the complete reduction of Pt particles. Hence, the actual content of cationic Pt species in various pre-oxidized Pt/TiO$_2$ catalysts should be lower than the XPS analysis results of the corresponding catalysts.

Likewise, another detail of the CO-DRIFTS should be concerning. All the catalysts show different proportions in band intensity assigned to the CO linearly adsorbed in the Pt step (2065 cm^{-1}) and terrace sites (2089 cm^{-1}), respectively. Obviously, the band intensities at 2065 cm^{-1} of the various catalysts gradually increase with increasing pre-oxidation temperature. These are intimately linked to the coordination structure of the surface Pt atoms. According to Hayden et al.'s research results [41], the stepped Pt site fraction of various catalysts could be calculated and the corresponding results are depicted in Figure 6b. The pristine Pt/TiO$_2$ catalyst contains 32% of stepped Pt site, whereas that of Pt/TiO$_2$ pre-oxidized at 300 °C increases to 39.4%. This demonstrates that mild pre-oxidation treatment could increase the step sites of the Pt nanoparticles of Pt/TiO$_2$.
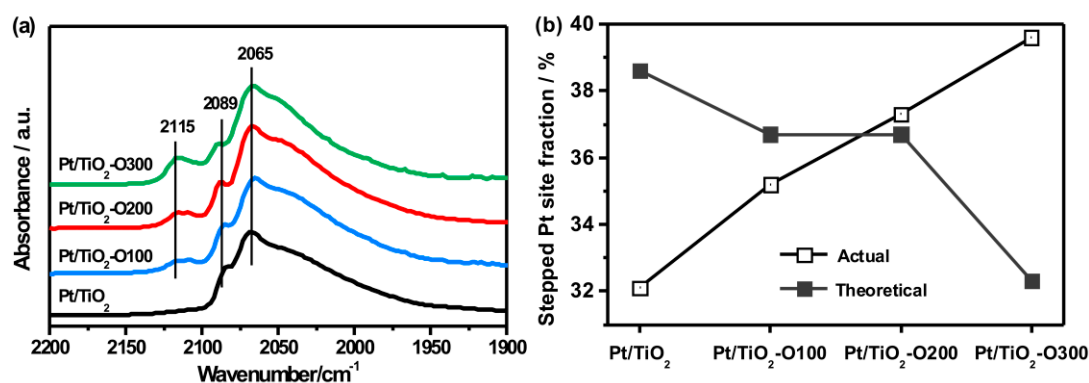

Figure 6. CO-DRIFT spectra (**a**) and stepped Pt site fraction (**b**) of various Pt/TiO$_2$ catalysts with different temperatures of pre-oxidation treatment. Note that the actual stepped Pt site fraction was calculated according to the equation, Fraction $= \frac{I_{2065}/\varepsilon}{I_{2065}/\varepsilon + I_{2089}}$, where I is the DRIFTS intensity and ε is a factor of 3.7. The theoretical stepped Pt site fraction is calculated by the Pt particle size according to the relationship observed in the literature [42].

Generally, the increasing curvature of the intact Pt particles means that the decreasing Pt particle size could lead to an increase in the fraction of the step site. Nevertheless, the above HRTEM analysis results have confirmed the increasing Pt particle size under the high temperature of the pre-oxidation treatment. Christopher et al. established the relationship of the Pt site fraction with the Pt particle size by virtue of the CO-DRIFTS and HRTEM analysis [42]. Accordingly, we calculated Pt site fraction based on our HRTEM analysis results and their corresponding results are also displayed in Figure 6b. It could be seen that the stepped Pt site fraction calculated from the HRTEM results shows a complete contrast variation trend to that from CO-DRIFTS. Thus, the increasing fraction of the step site of the pre-oxidized Pt/TiO$_2$ could not be attributed to the increasing Pt particle size. Theoretically, on an intact spherical surface, the decreasing Pt particle size is the unique consequence caused by the increasing fraction of the step site. However, augmentation in both stepped Pt site fractions and

their particle sizes illustrate that the intact spherical surface model is not responsible for the present results. That is to say, the spherical surface of the Pt particles of pre-oxidized catalysts is defective. The mild pre-oxidation treatment could increase the surface roughness of Pt particles. As shown in Figure 6b, the discrepancy between the actual and theoretical value is gradually largening with increasing pre-oxidation temperature, which suggests increasing the Pt surface roughness.

2.3. Structure-Performance Relationship Discussion

Generally, the HCHO decomposition performance of the catalysts could be influenced by numerous structural properties of supports and their corresponding active sites. From the above analysis, it is not difficult to find that the present mild pre-oxidation treatment has no influence on the TiO_2 structure. XRD and BET results have demonstrated the similarity in TiO_2 structure of Pt/TiO_2 catalysts with pre-oxidation at different temperatures. Obviously, the negligible structural distinction among these supports of catalysts is not responsible for their significantly different HCHO decomposition performances.

The following discussion is mainly focused on the influence of structural parameters of Pt nanoparticles on the low-temperature HCHO decomposition performance of various pre-oxidized Pt/TiO_2. HRTEM results (as seen in Figure 3) have showed that the Pt particle size slightly increases with the increasing temperature of the pre-oxidation treatment. Pt/TiO_2-O300 has the largest Pt particle size (3.1 nm), which is merely increased by 0.5 nm compared with that of the pristine Pt/TiO_2 (2.6 nm). Leung et al. systemically compared the influence of Pt particles on HCHO decomposition performance of Pt/TiO_2. They found that the the Pt/TiO_2 catalyst with a Pt particle size of 10.1 nm showed a similar HCHO conversion to that with 1.54 nm (70.6% vs. 71.5%) [13]. In this case, the HCHO decomposition activity of Pt/TiO_2-O200 is around three times as that of the pristine Pt/TiO_2, but both instead possess nearly the same Pt particle sizes (2.6 nm vs. 2.7 nm). Hence, the Pt particle size is not the main factor for influencing the HCHO decomposition performance of the pre-oxidized Pt/TiO_2 catalysts.

As for the influence of the chemical valence, the XPS and CO-DRIFTS results have proved the coexistence of metallic and cationic Pt species in various pre-oxidized Pt/TiO_2 catalysts. In terms of the monometallic catalyst, most of the research viewpoints support that the metallic species rather than the cationic one are the real active sites of the HCHO decomposition [11,16]. In this case, the pristine Pt/TiO_2 catalyst with the pure metallic Pt has the reactivity of low-temperature HCHO decomposition. Despite the coexistence of metallic and cationic Pt in all pre-oxidized Pt/TiO_2 catalysts, the high ratio of cationic Pt of Pt/TiO_2-O300 is not beneficial to its HCHO decomposition performance. Apparently, the present results seem to support the metallic Pt functional mechanism in Pt/TiO_2.

Besides increasing the cationic Pt content, mild pre-oxidation treatment also increases the fraction of stepped Pt sites and surface roughness of Pt nanoparticles. Theoretically, the stepped metal atoms, due to their under-coordinated characteristics, have superior ability to activate the adsorbed reactants in many reactions. This could achieve the fundamentally different catalytic consequence of the pre-oxidized Pt/TiO_2 catalyst [42–44]. Accordingly, it could explain the enhanced HCHO decomposition performance of the Pt/TiO_2 pre-oxidized at 100 °C and 200 °C. Pt/TiO_2-O300 has the highest fraction of stepped Pt sites, while it instead shows the lowest catalytic performance. Combined with above analysis of chemical valence, it is confirmed that the high temperature of pre-oxidation treatment gives rise to increasing the cationic Pt content. That leads to the increasing thickness or coverage of the cationic Pt layer over the metallic core [30]. Consequently, the quantity of active sites in the Pt/TiO_2-O300 correspondingly decreases even with the highest fraction of stepped Pt sites. Viewed by the structure of Pt particles, the mild temperature of preeoxidation treatment is essential for obtaining the enhanced HCHO decomposition performance of the Pt/TiO_2 catalyst.

Subsequently, the change in the activation and reaction mechanism of reactants brought by different structural Pt nanoparticles is studied in detail. Th eoxidizing agent and HCHO are two main reactants of low-temperature HCHO decomposition reaction. As mentioned above, O1s XPS analyses in Figure 5b and Table 2 have showed that the O_{II} content of all pre-oxidized Pt/TiO_2 catalysts are

obviously higher than that of the pristine Pt/TiO$_2$. The Pt/TiO$_2$-O200 catalyst possesses the highest O$_{II}$ content. It indicates that the pre-oxidation treatment could moderately increase the ability of oxygen activation of the Pt/TiO$_2$ catalyst. Generally, O$_{II}$ and OH$^-$ are considered to be the active species of HCHO decomposition reaction [10,11]. This could account for the excellent HCHO decomposition performance of Pt/TiO$_2$-O200. For OH$^-$, all pre-oxidized Pt/TiO$_2$ catalysts have significantly higher content than that of the pristine one. Actually, the pristine Pt/TiO$_2$ may have no ability of water dissociation due to its negligible OH$^-$ signal intensity. The OH$^-$ contents of the pre-oxidized Pt/TiO$_2$ catalysts decline with increasing pre-oxidation temperature. Consequently, the mild pre-oxidation treatment could effectively improve the activation of oxygen and hydroxyl of Pt/TiO$_2$.

The reaction process of HCHO is so complex because it contains many reaction steps and several intermediates [45,46]. It is crucial to understand the detailed contribution of mild pre-oxidation treatment of catalysts on their HCHO decompositions. Thus, we used HCHO-DRIFTS to subsequently study the change in the HCHO decomposition route on different pre-oxidized catalysts. Figure 7a–c show the representative HCHO-DRIFTS profiles of various Pt/TiO$_2$ catalysts, and all of them can be seen in Figure S1 of the supporting material. The HCHO decomposition mechanism could be clarified by the stepwise investigation of the reaction process under different atmospheres. It could be seen that the peaks of all the catalysts appear at 2846 cm^{-1}~2954 cm^{-1}, which is ascribed to υ(C-H) of dioxymethylene (DOM) [47]. It indicates that the HCHO molecules could be rapidly turned into DOM once being adsorbed onto the catalyst surface. The vibrations at 1575 cm^{-1} and 1360 cm^{-1} can be attributed to the presence of formate, which is the product of the DOM transformation [3,16]. Moreover, a series of vibrations that appear at ca. 2040 cm^{-1} correspond to υ (C = O) of adsorbed CO. This is considered to originate from the formate dehydrogenation [3,45]. To sum up, both pristine Pt/TiO$_2$ and various pre-oxidized Pt/TiO$_2$ catalysts follow the typical decomposition path of HCHO→DOM→formate→CO→CO$_2$.
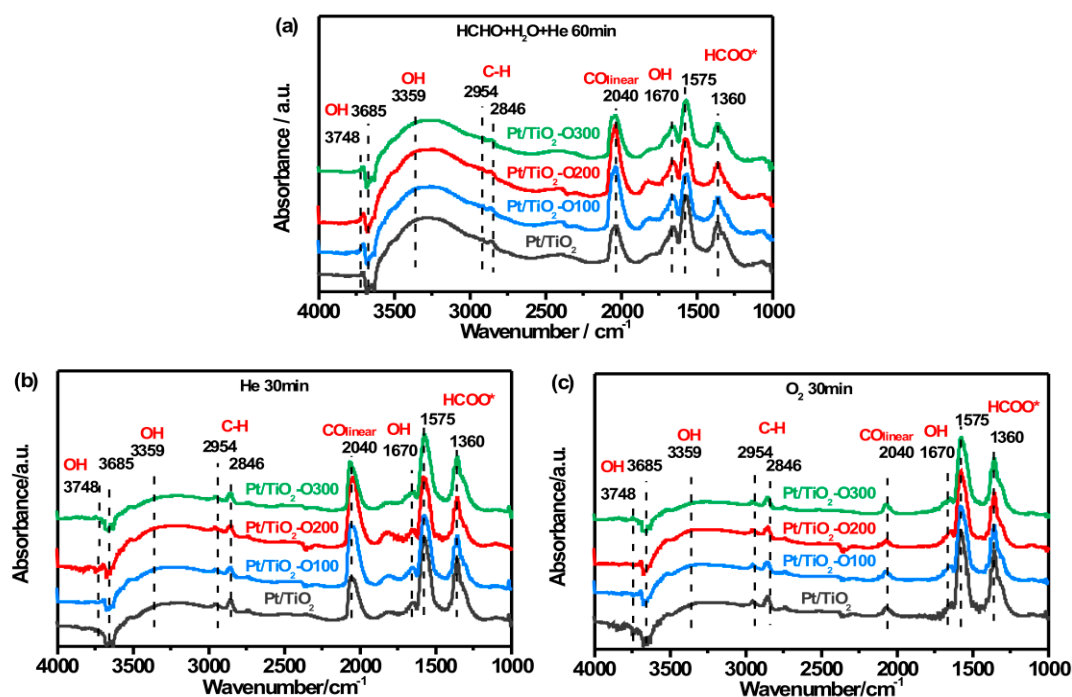

Figure 7. HCHO-DRIFT profiles of various pre-oxidized Pt/TiO$_2$ catalysts and pristine Pt/TiO$_2$ after (**a**) a flow of He + HCHO + H$_2$O for 60 min, (**b**) He purging for 30 min, and finally (**c**) O$_2$ purging for 30 min.

The signal intensity of two key intermediates, formate and CO, was countered as a function of time and atmosphere. As shown in Figure 8, various catalysts show distinctly different variation trends in the signal intensity of the intermediates. This suggests their varying reaction process of

HCHO decomposition, which could be responsible for their different catalytic performances. Figure 8a displays the signal intensity of formate as a function of time. It could be seen that the formate signal intensity in all catalysts shows a rapid increase at the initial stage of the HCHO + H_2O purge, and subsequently grows to their respective saturation value. In comparison, the pristine Pt/TiO_2 catalyst has slightly stronger formate signal intensity than that of the pre-oxidized ones. The differences in formate signal intensity among the pre-oxidized Pt/TiO_2 catalysts are not significant. At the second stage, the atmosphere of the in situ chamber is switched into pure He. The formate signal intensity in all catalysts increases, indicating the continuous transformation of DOM into formate in this stage. After pure oxygen purging, all the catalysts maintain a constant formate signal intensity.

Figure 8. Signal Intensities of formate (**a**) and CO (**b**) as a function of time and atmosphere over the pristine Pt/TiO_2 catalyst and the pre-oxidized Pt/TiO_2 catalysts.

Furthermore, Figure 8b shows the change in signal intensity of CO as a function of time. At the first stage, CO signal intensities of various catalysts, as analogous to formate signal variation, gradually increase to their respective saturation values. All catalysts maintain the constant CO signal intensity at the second stage of pure He purging. At the third stage, CO signal intensity of catalysts rapidly declines to a very low value once oxygen is injected into the in situ cell. This indicates the easy oxidation of adsorbed CO molecules on various Pt/TiO_2 catalysts. Noteworthy is that the increased speed in CO signal intensity of all catalysts is observably slower than that in the formate signal intensity. It demonstrates the relatively slow dehydrogenation rate of formate compared with that of further CO oxidation. As reported in numerous studies, formate dehydrogenation to CO is the rate-determining step of low-temperature HCHO decomposition [3,4]. Moreover, CO signal intensities at the first and second stages are obviously different in these Pt/TiO_2 catalysts. Among them, Pt/TiO_2-O100 and Pt/TiO_2-O200 show relatively higher CO signal intensities compared with that of Pt/TiO_2-O300 and pristine Pt/TiO_2. This indicates the rapid formate dehydrogenation to CO, which could be responsible for their excellent HCHO decomposition performance of mild pre-oxidized Pt/TiO_2 catalysts.

Based on the results and discussion mentioned above, we can clarify the relationship between mild pre-oxidation treatment and HCHO decomposition performance of the Pt/TiO_2 catalyst. The mild pre-oxidation treatment mainly influences the structure of the Pt nanoparticles rather than that of the catalyst support. Metallic and cationic Pt species coexist and the surface roughness of Pt nanoparticles increases in various pre-oxidized Pt/TiO_2 catalysts. Correspondingly, pre-oxidized Pt/TiO_2 catalysts could have enhanced performance of oxygen activation and water dissociation. Further, pre-oxidation treatment is confirmed to accelerate the formate dehydrogenation to CO, which improves the HCHO decomposition performance of the pre-oxidized Pt/TiO_2 catalyst. Of course, the temperature of pre-oxidation treatment is very important for the catalytic performance of the catalyst. If placed in too high temperature, the obtained preeoxidized Pt/TiO_2 catalyst could instead have weakened performance of oxygen activation and water dissociation. Therefore, pre-oxidation treatment under a mild station is crucial for achieving the excellent low-temperature HCHO decomposition performance of the Pt/TiO_2 catalyst.

3. Materials and Methods

3.1. Chemicals and Synthesis

Chloroplatinic acid ($H_2PtCl_6 \cdot 6H_2O$, CAS: 16941-12-1, Shanghai Agent Co., Ltd. Shangai, China), chloroauric acid ($HAuCl_4 \cdot 4H_2O$, Shanghai Agent Co., Ltd.), sodium hydroxide (NaOH, CAS: 1310-73-2, Nanjing Agent Co., Ltd. Nanjing, China), silicon dioxide (SiO_2, A380, CAS: 112 945-52-5, Evonik Degussa Co., Ltd., Essen, Germany), and titania (TiO_2, Xuancheng Jingrui New Material Co., Ltd.) were used as received.

The Pt/TiO_2 catalyst was prepared by the conventional method of wetness impregnation. 0.64 mL of H_2PtCl_6 aqueous solution (0.0386 mol/L) was added by drops into 1 g of TiO_2 powder with slow stirring. After standing for 12 h, the paste was dried in a vacuum oven at 110 °C for 6 h. The powders were calcined at 500 °C for 2 h in air atmosphere, and then were reduced in a H_2 atmosphere for 2 h at 300 °C. Finally, the Pt/TiO_2 catalyst with 0.5 wt.% of Pt loading amount could be achieved, which needed to be kept in a vacuum dryer.

The mild pre-oxidation treatment of Pt/TiO_2 was carried out in pure O_2 atmosphere. 0.4 g of the aforementioned Pt/TiO_2 catalyst was filled in a quartz tube (inner diameter: 10 mm) of furnace. The flow rate of pure O_2 was 50 mL/min. Then, the temperature of the furnace was increased from room temperature to specified pretreatment temperature at an increasing rate of 5 °C/min. After maintaining 0.5 h, the temperature of the furnace was decreased to room temperature. The obtained pretreated Pt/TiO_2 catalyst was entitled as Pt/TiO_2-Ox, where x represented the pretreatment temperature.

3.2. Characterization

The information in the crystal phase of various catalysts was analyzed by a D8-Advance X-ray Diffractometer (Bruker) by Cu Kα radiation (λ = 0.1542 nm) at a scanning rate of 10 °/min and with a step size of 0.02°. The analysis of the porous structure of various catalysts was performed on ASAP2020 system (Micromeritics) at −196 °C. Surface area (S_{BET}) and pore volume (V_P) were achieved by the BET method and nitrogen adsorption at a relative pressure of 0.99, respectively. The average pore size (D_P) was calculated from the adsorption isotherm according to the Barrett-Joyner-Halenda (BJH) method. The morphological information of the Pt particles and the corresponding size distribution of the catalyst were obtained by high-resolution transmission electron microscopy (HRTEM) on a JEM-2010 UHR microscope (JEOL) at 200 kV. The dispersion state of the Pt element in Pt/TiO_2 catalyst was characterized by scanning transmission electron microscopy (STEM)-high-angle annular dark-field (HAADF) and energy-dispersive X-ray spectroscopy (EDX). This was performed on a JEOL JEM-2100Plus at an accelerating voltage of 200 kV. The valent state of various elements on the catalyst surface was identified on a ESCALAB 250 X-ray Photoelectron Spectrometer (XPS), which was operated at a pass energy of 30 eV, using Al Kα (λ = 1486.7 eV) as an exciting X-ray source. All spectra were calibrated as reference to the binding energy of C1s line at 284.8 eV. Temperature programmed oxidation (TPO) experiments were conducted by using the TP-5000 equipment. The reduced Pt/TiO_2 catalyst was pretreated by 10% H_2/N_2 at 300 °C for 0.5 h, and subsequently oxidized by pure O_2 to imitate the atmosphere of the pre-oxidation treatment from room temperature up to 500 °C at a rate of 10 °C/min. Moreover, the temperature programmed reduction (TPR) experiments were also carried out on TP-5000 equipment. The unreduced Pt/TiO_2 was the starting sample for TPR analysis. Followed by being in situ and pretreated by pure He atmosphere at 300 °C for 0.5 h, the sample was purged with 10% H_2/N_2 at room temperature ~500 °C and the corresponding off-gas signal was recorded. In situ diffuse reflectance infrared Fourier transform spectroscopy (DRIFTS) was carried out on a Nicolet 6700 spectroscope apparatus (Thermo Electron, Waltham, MA, USA) equipped with a diffuse reflectance accessory and a mercury-cadmium-telluride (MCT) detector. The experimental processes of CO-DRIFTs were shown as follows: the catalyst powder was placed into a copper crucible of in-situ chamber. Firstly, the catalyst was pretreated in a pure He flow (30 mL/min) at 300 °C for 0.5 h with a heating rate of 10 °C/min and cooled down to room temperature. Secondly, 1% CO/He was introduced into the chamber. After 0.5 h,

the atmosphere of the chamber was switched to pure He again to avoid the interference of gaseous CO. Finally, the CO absorbed spectrum of the catalyst could be achieved. For the HCHO-DRIFTS experiment, the pretreated samples also needed to experience three periods. Initially, HCHO was bubbled into the chamber with He (ca. 35% of relative humidity) at 30 °C. Subsequently, after 1 h, the chamber was purged with pure He and kept for 0.5 h. Plus, 20% O_2/He, instead of pure He, was introduced into the chamber. The spectra with different periods were recorded after 32 scans with a resolution of 4 cm^{-1}.

3.3. Catalytic Activity Tests

The HCHO decomposition performance of various catalysts was evaluated in a fixed bed flow reactor. 0.1 g of the catalyst powders were laid in the quartz tube (8 mm). Then, a mixed feed gas was injected into quartz tube and the total flow containing gaseous 320 ppm HCHO, 20 vol.% O_2 and balanced gas (N_2). The relative humidity of the feed gas was around 35%. The whole gas velocity of the HCHO conversion and stability test was controlled at 45000 mL/(h·g). The experimental process for calculating reaction rate of catalysts was carried out at the whole gas velocity of 90000 mL/(h·g). The exhaust CO_2 concentration was analyzed online by a CO_2 gas analyzer to achieve the HCHO conversion of catalysts.

4. Conclusions

The present work reported a mild pre-oxidation approach to improve the low-temperature HCHO decomposition of typical Pt/TiO$_2$ catalyst. The optimized HCHO decomposition activity of the pre-oxidized Pt/TiO$_2$ was around three times that of the pristine one. The pre-oxidation treatment did not significantly change the structure of the support TiO$_2$ and Pt particle size of various catalysts. Both cationic Pt content and roughness of Pt particles increase in the pre-oxidized Pt/TiO$_2$ catalysts, and their performances of oxygen activation and water dissociation were improved. Moreover, the mild pre-oxidation could obviously accelerate the formate dehydrogenation to CO in pre-oxidized Pt/TiO$_2$ catalysts.

References

1. Bianchi, F.; Careri, M.; Musci, M.; Mangia, A. Fish and food safety: Determination of formaldehyde in 12 fish species by SPME extraction and GC–MS analysis. *Food Chem.* **2007**, *100*, 1049–1053. [CrossRef]
2. Salthammer, T.; Mentese, S.; Marutzky, R. Formaldehyde in the indoor environment. *Chem. Rev.* **2010**, *110*, 2536–2572. [CrossRef] [PubMed]
3. Zhang, C.; He, H.; Tanaka, K.-I. Catalytic performance and mechanism of a Pt/TiO$_2$ catalyst for the oxidation of formaldehyde at room temperature. *Appl. Catal. B Environ.* **2006**, *65*, 37–43. [CrossRef]
4. Zhang, C.; Liu, F.; Zhai, Y.; Ariga, H.; Yi, N.; Liu, Y.; Asakura, K.; Flytzani-Stephanopoulos, M.; He, H. Alkali-metal-promoted Pt/TiO$_2$ opens a more efficient pathway to formaldehyde oxidation at ambient temperatures. *Angew. Chem. Int. Ed.* **2012**, *51*, 9628–9632. [CrossRef] [PubMed]

5. Wang, L.; Tran, T.P.; Vo, D.V.; Sakurai, M.; Kameyama, H. Design of novel Pt-structured catalyst on anodic aluminum support for VOC's catalytic combustion. *Appl. Catal. A Gen.* **2008**, *350*, 150–156. [CrossRef]

6. Li, Y.; Zhang, C.; He, H.; Zhang, J.; Chen, M. Influence of alkali metals on Pd/TiO$_2$ catalysts for catalytic oxidation of formaldehyde at room temperature. *Catal. Sci. Technol.* **2016**, *6*, 2289–2295. [CrossRef]

7. Sun, X.; Lin, J.; Guan, H.; Li, L.; Sun, L.; Wang, Y.; Miao, S.; Su, Y.; Wang, X. Complete oxidation of formaldehyde over TiO$_2$ supported subnanometer Rh catalyst at ambient temperature. *Appl. Catal. B Environ.* **2018**, *226*, 575–584. [CrossRef]

8. Zhu, L.; Jacob, D.J.; Keutsch, F.N.; Mickley, L.J.; Scheffe, R.; Strum, M.; González Abad, G.; Chance, K.; Yang, K.; Rappenglück, B. Formaldehyde (HCHO) as a hazardous air pollutant: Mapping surface air concentrations from satellite and inferring cancer risks in the United States. *Environ. Sci. Technol.* **2017**, *51*, 5650–5657. [CrossRef]

9. Al Soubaihi, R.; Saoud, K.; Dutta, J. Critical Review of Low-Temperature CO Oxidation and Hysteresis Phenomenon on Heterogeneous Catalysts. *Catalysts* **2018**, *8*, 660. [CrossRef]

10. Nie, L.; Yu, J.; Jaroniec, M.; Tao, F.F. Room-temperature catalytic oxidation of formaldehyde on catalysts. *Catal. Sci. Technol.* **2016**, *6*, 3649–3669. [CrossRef]

11. Guo, J.; Lin, C.; Jiang, C.; Zhang, P. Review on noble metal-based catalysts for formaldehyde oxidation at room temperature. *Appl. Surf. Sci.* **2019**, *475*, 237–255. [CrossRef]

12. Bai, B.; Qiao, Q.; Li, J.; Hao, J. Progress in research on catalysts for catalytic oxidation of formaldehyde. *Chin. J. Catal.* **2016**, *37*, 102–122. [CrossRef]

13. Huang, H.; Hu, P.; Huang, H.; Chen, J.; Ye, X.; Leung, D.Y. Highly dispersed and active supported Pt nanoparticles for gaseous formaldehyde oxidation: Influence of particle size. *Chem. Eng. J.* **2014**, *252*, 320–326. [CrossRef]

14. An, N.; Zhang, W.; Yuan, X.; Pan, B.; Liu, G.; Jia, M.; Yan, W.; Zhang, W. Catalytic oxidation of formaldehyde over different silica supported platinum catalysts. *Chem. Eng. J.* **2013**, *215*, 1–6. [CrossRef]

15. An, N.; Yu, Q.; Liu, G.; Li, S.; Jia, M.; Zhang, W. Complete oxidation of formaldehyde at ambient temperature over supported Pt/Fe2O3 catalysts prepared by colloid-deposition method. *J. Hazard. Mater.* **2011**, *186*, 1392–1397. [CrossRef] [PubMed]

16. Huang, H.; Leung, D.Y.; Ye, D. Effect of reduction treatment on structural properties of TiO$_2$ supported Pt nanoparticles and their catalytic activity for formaldehyde oxidation. *J. Mater. Chem.* **2011**, *21*, 9647–9652. [CrossRef]

17. Yan, Z.; Xu, Z.; Yu, J.; Jaroniec, M. Highly active mesoporous ferrihydrite supported Pt catalyst for formaldehyde removal at room temperature. *Environ. Sci. Technol.* **2015**, *49*, 6637–6644. [CrossRef] [PubMed]

18. Peng, J.; Wang, S. Correlation between microstructure and performance of Pt/TiO$_2$ catalysts for formaldehyde catalytic oxidation at ambient temperature: effects of hydrogen pretreatment. *J. Phys. Chem. C* **2007**, *111*, 9897–9904. [CrossRef]

19. Xu, F.; Le, Y.; Cheng, B.; Jiang, C. Effect of calcination temperature on formaldehyde oxidation performance of Pt/TiO$_2$ nanofiber composite at room temperature. *Appl. Surf. Sci.* **2017**, *426*, 333–341. [CrossRef]

20. Li, L.; Yue, H.; Zhang, S.; Huang, Y.; Zhang, W.; Wu, P.; Ji, Y.; Huo, F. Solving the Water Hypersensitive Challenge of Sulfated Solid Superacid in Acid-Catalyzed Reactions. *ACS Appl. Mater. Interfaces* **2019**, *11*, 9919–9924. [CrossRef] [PubMed]

21. Wu, H.-C.; Chen, T.-C.; Chen, Y.-C.; Lee, J.-F.; Chen, C.-S. Formaldehyde oxidation on silica-supported Pt catalysts: The influence of thermal pretreatments on particle formation and on oxidation mechanism. *J. Catal.* **2017**, *355*, 87–100. [CrossRef]

22. Li, Y.; Zhang, C.; Ma, J.; Chen, M.; Deng, H.; He, H. High temperature reduction dramatically promotes Pd/TiO$_2$ catalyst for ambient formaldehyde oxidation. *Appl. Catal. B Environ.* **2017**, *217*, 560–569. [CrossRef]

23. Zhu, L.; Wang, J.; Rong, S.; Wang, H.; Zhang, P. Cerium modified birnessite-type MnO$_2$ for gaseous formaldehyde oxidation at low temperature. *Appl. Catal. B Environ.* **2017**, *211*, 212–221. [CrossRef]

24. Alayon, E.; Singh, J.; Nachtegaal, M.; Harfouche, M.; van Bokhoven, J.A. On highly active partially oxidized platinum in carbon monoxide oxidation over supported platinum catalysts. *J. Catal.* **2009**, *263*, 228–238. [CrossRef]

25. Ke, J.; Zhu, W.; Jiang, Y.; Si, R.; Wang, Y.-J.; Li, S.-C.; Jin, C.; Liu, H.; Song, W.-G.; Yan, C.-H. Strong Local Coordination Structure Effects on Subnanometer PtOx Clusters over CeO$_2$ Nanowires Probed by Low-Temperature CO Oxidation. *ACS Catal.* **2015**, *5*, 5164–5173. [CrossRef]

26. Parayil, S.K.; Kibombo, H.S.; Wu, C.-M.; Peng, R.; Kindle, T.; Mishra, S.; Ahrenkiel, S.P.; Baltrusaitis, J.; Dimitrijevic, N.M.; Rajh, T. Synthesis-dependent oxidation state of platinum on TiO$_2$ and their influences on the solar simulated photocatalytic hydrogen production from water. *J. Phys. Chem. C* **2013**, *117*, 16850–16862. [CrossRef]

27. Kuhaudomlap, S.; Mekasuwandumrong, O.; Praserthdam, P.; Fujita, S.-I.; Arai, M.; Panpranot, J. The H$_2$-Treated TiO$_2$ Supported Pt Catalysts Prepared by Strong Electrostatic Adsorption for Liquid-Phase Selective Hydrogenation. *Catalysts* **2018**, *8*, 87. [CrossRef]

28. Li, M.; Song, J.; Yue, F.; Pan, F.; Yan, W.; Hua, Z.; Li, L.; Yang, Z.; Li, L.; Wen, G. Complete Hydrodesulfurization of Dibenzothiophene via Direct Desulfurization Pathway over Mesoporous TiO$_2$-Supported NiMo Catalyst Incorporated with Potassium. *Catalysts* **2019**, *9*, 448. [CrossRef]

29. Li, L.; Yue, H.; Ji, T.; Li, W.; Zhao, X.; Wang, L.; She, J.; Gu, X.; Li, X. Novel mesoporous TiO$_2$(B) whisker-supported sulfated solid superacid with unique acid characteristics and catalytic performances. *Appl. Catal. A Gen.* **2019**, *574*, 25–32. [CrossRef]

30. Huizinga, T.; Van Grondelle, J.; Prins, R. A temperature programmed reduction study of Pt on Al$_2$O$_3$ and TiO$_2$. *Appl. catal.* **1984**, *10*, 199–213. [CrossRef]

31. Zhu, X.; Shen, M.; Lobban, L.L.; Mallinson, R.G. Structural effects of Na promotion for high water gas shift activity on Pt–Na/TiO$_2$. *J. Catal.* **2011**, *278*, 123–132. [CrossRef]

32. Wang, L.; Sakurai, M.; Kameyama, H. Study of catalytic decomposition of formaldehyde on Pt/TiO$_2$ alumite catalyst at ambient temperature. *J. Hazard. Mater.* **2009**, *167*, 399–405. [CrossRef] [PubMed]

33. Epling, W.S.; Cheekatamarla, P.K.; Lane, A.M. Reaction and surface characterization studies of titania-supported Co, Pt and Co/Pt catalysts for the selective oxidation of CO in H$_2$-containing streams. *Chem. Eng. J.* **2003**, *93*, 61–68. [CrossRef]

34. Huang, H.; Leung, D.Y. Complete elimination of indoor formaldehyde over supported Pt catalysts with extremely low Pt content at ambient temperature. *J. Catal.* **2011**, *280*, 60–67. [CrossRef]

35. Wang, W.; Chen, X.; Cai, Q.; Mo, G.; Jiang, L.; Zhang, K.; Chen, Z.; Wu, Z.; Pan, W. In situ SAXS study on size changes of platinum nanoparticles with temperature. *Eur. Phys. J. B* **2008**, *65*, 57–64. [CrossRef]

36. Ono, L.; Yuan, B.; Heinrich, H.; Cuenya, B.R. Formation and thermal stability of platinum oxides on size-selected platinum nanoparticles: support effects. *J. Phys. Chem. C* **2010**, *114*, 22119–22133. [CrossRef]

37. Vovk, E.I.; Kalinkin, A.V.; Smirnov, M.Y.; Klembovskii, I.O.; Bukhtiyarov, V.I. XPS study of stability and reactivity of oxidized Pt nanoparticles supported on TiO$_2$. *J. Phys. Chem. C* **2017**, *121*, 17297–17304. [CrossRef]

38. Ruiz-Martínez, J.; Sepúlveda-Escribano, A.; Anderson, J.A.; Rodríguez-Reinoso, F. Spectroscopic and microcalorimetric study of a TiO$_2$-supported platinum catalyst. *Phys. Chem. Chem. Phys.* **2009**, *11*, 917–920. [CrossRef] [PubMed]

39. Panagiotopoulou, P.; Kondarides, D.I. Effects of alkali additives on the physicochemical characteristics and chemisorptive properties of Pt/TiO$_2$ catalysts. *J. Catal.* **2008**, *260*, 141–149. [CrossRef]

40. Panagiotopoulou, P.; Christodoulakis, A.; Kondarides, D.; Boghosian, S. Particle size effects on the reducibility of titanium dioxide and its relation to the water–gas shift activity of Pt/TiO$_2$ catalysts. *J. Catal.* **2006**, *240*, 114–125. [CrossRef]

41. Hayden, B.; Kretzschmar, K.; Bradshaw, A.; Greenler, R. An infrared study of the adsorption of CO on a stepped platinum surface. *Surf. Sci.* **1985**, *149*, 394–406. [CrossRef]

42. Kale, M.J.; Christopher, P. Utilizing quantitative in situ FTIR spectroscopy to identify well-coordinated Pt atoms as the active site for CO oxidation on Al$_2$O$_3$-supported Pt catalysts. *ACS Catal.* **2016**, *6*, 5599–5609. [CrossRef]

43. Wang, C.; Ouyang, M.; Li, M.; Lee, S.; Flytzani-Stephanopoulos, M. Low-Coordinated Pd Catalysts Supported on Zn1Zr1Ox Composite Oxides for Selective Methanol Steam Reforming. *Appl. Catal. A Gen.* **2019**, *580*, 81–92. [CrossRef]

44. Qiu, C.; Zhao, C.; Sun, X.; Deng, S.; Zhuang, G.; Zhong, X.; Wei, Z.; Yao, Z.; Wang, J.-g. Multiscale Simulation of Morphology Evolution of Supported Pt Nanoparticles via Interfacial Control. *Langmuir* **2019**, *35*, 6393–6402. [CrossRef] [PubMed]

45. Zhang, C.; He, H. A comparative study of TiO$_2$ supported noble metal catalysts for the oxidation of formaldehyde at room temperature. *Catalysis Today* **2007**, *126*, 345–350. [CrossRef]

46. Li, S.; Lu, X.; Guo, W.; Zhu, H.; Li, M.; Zhao, L.; Li, Y.; Shan, H. Formaldehyde oxidation on the Pt/TiO$_2$(101) surface: A DFT investigation. *J. Organomet. Chem.* **2012**, *704*, 38–48. [CrossRef]

47. Mao, C.-F.; Vannice, M.A. Formaldehyde oxidation over Ag catalysts. *J. Catal.* **1995**, *154*, 230–244. [CrossRef]